International Journal of Aeronautical and Space Sciences (2025) 26:2695–2711
https://doi.org/10.1007/s42405-025-00904-y

IJASS International Journal of Aeronautical and Space Sciences

ORIGINAL PAPER

Spacecraft Attitude Control with On-Off Thrusters via Convex Optimization Based Control Allocation

Jibon Kim[1] · Jong-Han Kim[1]

Received: 31 July 2024 / Revised: 23 November 2024 / Accepted: 27 January 2025 / Published online: 14 February 2025

Abstract
This paper presents a comprehensive study on the development and evaluation of an advanced control allocation algorithm for spacecraft attitude control, utilizing linear programming (LP) and relaxed quadratic programming (QP). The focus of this research is on optimizing the distribution of control forces among thrusters within the reaction control system (RCS) to enhance the precision and efficiency of spacecraft orientation maneuvers. The challenge of control allocation is addressed through an optimization framework that integrates multi-objective functions, which are solved using sophisticated convex optimization techniques. Detailed numerical experiments were conducted to assess the effectiveness of the proposed methods under varying operational conditions, ranging from straightforward to highly demanding. The findings demonstrate that both LP and relaxed QP are capable of effectively stabilizing the spacecraft's attitude and angular velocity, with relaxed QP showing superior adaptability in handling more extreme conditions. These experiments confirmed the robustness, efficiency, and stability of the control strategies across a broad spectrum of scenarios. The successful application of these control strategies highlights their potential to significantly enhance the operational reliability and efficiency of spacecraft missions.

Keywords Attitude control · Control allocation · Convex optimization

1 Introduction

Attitude control is a fundamental aspect of spacecraft functionality, playing a critical role in the mission success and operational efficiency of space-based platforms. Precise attitude control is imperative, as it ensures that a spacecraft's instruments and sensors maintain the correct orientation towards their intended targets, whether those are terrestrial, other celestial bodies, or the vast expanse of deep space. This precision directly influences the quality and reliability of data acquisition activities that span scientific observations, Earth imaging, and telecommunications.

Furthermore, maintaining the correct orientation facilitates efficient power generation from solar panels, optimizes thermal control systems, and is crucial for the successful execution of complex docking and maneuvering operations. Reflecting its importance, extensive research has been devoted to refining the mechanisms of spacecraft attitude control. These systems aim to minimize propellant consumption for corrective maneuvers, thereby extending the operational lifespan of spacecraft and reducing overall mission costs [1–3].

Among the various technologies employed to maintain spacecraft orientation, reaction control systems (RCS) play a pivotal role. RCS typically comprises multiple thrusters that produce precise, controlled bursts of force to adjust the spacecraft's orientation and position [4, 5]. The effectiveness of RCS hinges on accurate control force allocation-optimally distributing thrust among the thrusters to achieve the desired torque and force outcomes. This process must minimize fuel consumption and ensure the stability of the spacecraft under the dynamic conditions of space, involving sophisticated algorithms and robust control strategies [6–8].

As the number of thrusters increases, so too does the complexity of control allocation. This increase has spurred a wealth of research aimed at developing more effective control allocation strategies that can cope with the demands of advanced spacecraft operations [9–12]. This paper introduces

Communicated by Hyuk Park.

✉ Jong-Han Kim
jonghank@inha.ac.kr

Jibon Kim
jibonkim@inha.edu

[1] Department of Aerospace Engineering, Inha University, Incheon, Republic of Korea

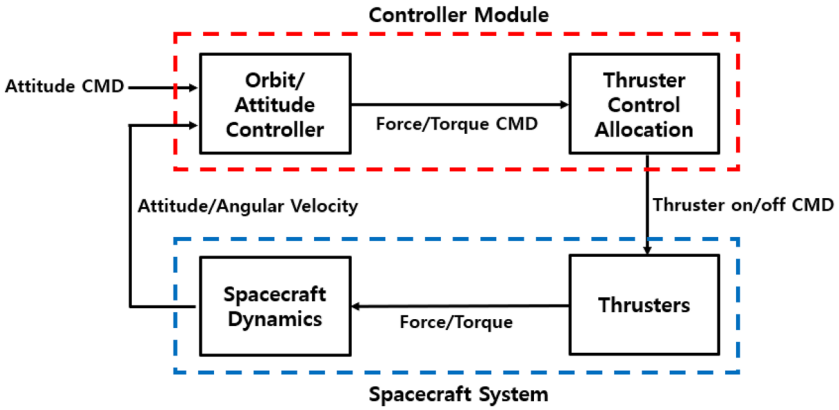

Fig. 1 Spacecraft attitude control systems with thrusters

an approach that employs advanced convex optimization techniques to facilitate rapid, efficient, and highly effective control allocation. By embracing the principles of convex optimization, our methodology not only streamlines the computational process but also enhances the accuracy and efficacy of control allocation, regardless of the number of thrusters involved. Convex optimization is essential for our application because it ensures robust handling of the complex constraints typical in spacecraft control systems, and supports the scalability required for managing multiple thrusters efficiently [13]. However, the optimization techniques employed in referenced papers [9–12] primarily utilize pseudo-inverse-based methods. These methods often become increasingly challenging to solve as more constraints are added. In contrast, convex optimization techniques, such as those employed in our approach, can efficiently handle a large number of constraints, provided that these constraints are convex. Moreover, convex problems can be solved with high efficiency using methods such as primal-dual interior point methods. Additionally, when the problem is formulated as a Quadratic Programming (QP) problem, as proposed in this paper, it can accommodate a variety of practical operational considerations. These include limiting the number of thrusters in use, balancing the usage among thrusters, and other relevant operational parameters.

In this paper, we demonstrated two key advantages of our relaxed QP approach. First, the proposed QP method overcomes the infeasibility issues encountered by the pseudo-inverse or LP approaches when excessive force/torque commands are required. Second, by employing the ℓ_1 regularizer, the relaxed QP approach effectively reduces the number of thrusters utilized while reliably generating the required force/torque commands.

Moreover, the control allocation methodology proposed in this paper is designed to mitigate the impact on the spacecraft's trajectories, even when applied to asymmetric thruster configurations. This capability underscores the adaptability of our algorithm, ensuring comprehensive attitude control across various configurations of thrusters. The robustness of this approach makes it highly suitable for diverse spacecraft designs, delivering reliable performance and maintaining the intended orbital trajectory without significantly perturbing it.

The structure of this paper is designed to provide a thorough exploration of our research on control allocation for spacecraft attitude control. Section 2 provides a detailed introduction to the thrusters and the dynamics of the spacecraft, offering a comprehensive overview of the physical systems that we consider. Section 3 delves into the quaternion feedback attitude controller and our novel control allocation algorithm, elucidating both the theoretical underpinnings and the practical applications of these strategies. Section 4 presents rigorous numerical simulations that integrate the models and algorithms previously introduced, followed by an in-depth analysis of the resulting data. The final section, Sect. 5, concludes the paper, summarizing our key findings and discussing their broader implications for ongoing research and operational applications in the field of spacecraft attitude control.

2 Spacecraft Systems

The spacecraft attitude control system is divided into two primary components: the controller module and the spacecraft system. The controller module includes the attitude controller and the control allocation algorithm, which are crucial for managing the orientation and stability of the spacecraft. The spacecraft system consists of the spacecraft dynamics and the thrusters, both essential for executing the physical maneuvers required by the controller module's commands.

Figure 1 presents a block diagram that illustrates the intricate structure of the spacecraft attitude control system. This diagram serves as an illustrative guide to understanding how commands are processed and executed within the system. The Spacecraft Systems, depicted in the diagram, receives specific commands for individual thrusters. These commands change the spacecraft's angular velocity, attitude, and velocity, thereby influencing its trajectory and positioning in space.

Within the Spacecraft Systems, there are two key subsystems: Spacecraft Dynamics and Thrusters. The Spacecraft Dynamics subsystem encompasses the equations and models that describe both translational and rotational motions of the spacecraft, integrating complex physics that governs how the spacecraft moves through space. The Thrusters subsystem plays a pivotal role by generating the necessary forces and torques. These thrusters operate based on on-off commands, which allows for precise control over the spacecraft's movements, ensuring that it can respond dynamically to the operational demands of its mission.

2.1 Thrusters

2.1.1 Force and Torque Generation via Thruster Actions

The thrusters of a spacecraft are typically mounted at fixed locations on the spacecraft's body. The configuration for the particular spacecraft considered in this paper arranges four thrusters on each face of a cubic structure, as depicted in Fig. 2. While the magnitude of the torque generated by these thrusters cannot be directly controlled, the angular momentum they produce can be controlled by adjusting the thrusters' on-time, a method known as duty-cycle control. The principle of duty-cycle control, which does not directly control the torque magnitude but instead matches the angular momentum achieved at the control time step through on-time adjustments, is illustrated in Fig. 3. For instance, if the available torque magnitude is twice the required torque, the thrusters would operate for only half the time step to achieve the necessary angular momentum. Each thruster is assumed to be individually controllable. Also, it is assumed that thruster activation coincides with the start of each control period, generating thrust of a constant magnitude immediately without any time delay.

The following derives the linear model for the thrust actuation [14]. The thrust actuation model is used not only to calculate the forces and torques acting on the spacecraft dynamics within the Spacecraft System module, but also in the control allocation algorithm. A linear model is constructed using the position vector and the thrust vector of the thrusters. As shown in Fig. 2, the position vector of the i-th thruster is denoted as $\mathbf{l_i}$ and the applied thrust vector is denoted as $\mathbf{F_i}$. The thruster configuration matrix can be expressed as follows.

$$\begin{bmatrix} \mathbf{F} \\ \boldsymbol{\tau} \end{bmatrix} = \underbrace{\begin{bmatrix} \mathbf{F_1} & \cdots & \mathbf{F_n} \\ \mathbf{l_1} \times \mathbf{F_1} & \cdots & \mathbf{l_n} \times \mathbf{F_n} \end{bmatrix}}_{A} \underbrace{\begin{bmatrix} u_1 \\ \vdots \\ u_n \end{bmatrix}}_{\mathbf{u}} \tag{1}$$

The upper three rows of the configuration matrix A compute the force vectors acting on the spacecraft from the individual thrusters, while the lower three rows calculate the torque vectors. If the thrusters were capable of generating continuous thrust, the vector $\mathbf{u}$ would represent the thrust magnitudes produced by the individual thrusters, normalized to the maximum thrust. However, in our formulation, $\mathbf{u}$ represents the on-time of the thrusters, consistent with duty-cycle control used with on-off thrusters.

Therefore, the computation $A\mathbf{u}$ yields the changes in linear momentum, denoted as $\mathbf{F}$, achieved by the thrusts applied during the time step Δt. Similarly, the lower three rows compute the changes in angular momentum, denoted as $\boldsymbol{\tau}$, achieved during the same interval.

2.2 Spacecraft Dynamics

2.2.1 Attitude Dynamics

Attitude dynamics consist of the differential equations that compute the time derivatives of the attitude and angular velocity of the spacecraft, utilizing the applied torques and current attitude [15]. This paper considers the general case of a rigid spacecraft rotating under the influence of body-fixed torque devices. Before delving into the dynamics, the reference frames used throughout this study are summarized in Table 1. In our analysis, attitude propagation is performed using quaternions, which are mathematical constructs that provide a compact and robust method for representing orientations and rotations in three-dimensional space. Quaternions are particularly advantageous for computational efficiency and avoiding the singularities associated with other representations like Euler angles. The quaternion attitude propagation equation is represented as follows:

$$\begin{aligned} \dot{\mathbf{q}}^{B_I} &= \frac{1}{2}\Omega(\boldsymbol{\omega}^{B}_{B/I})\mathbf{q}^{\mathbf{B}}_{\mathbf{I}}, \\ \Omega(\mathbf{x}) &= \begin{bmatrix} [\mathbf{x}\times] & \mathbf{x} \\ -\mathbf{x}^T & 0 \end{bmatrix}, \quad [\mathbf{x}\times] = \begin{bmatrix} 0 & -x_3 & x_2 \\ x_3 & 0 & -x_1 \\ -x_2 & x_1 & 0 \end{bmatrix}, \end{aligned} \tag{2}$$

where $\mathbf{q}^{\mathbf{B}}_{\mathbf{I}}$ denotes the quaternion representing the attitude of the Body frame (B-Frame) relative to the Inertial frame (I-Frame), and $\boldsymbol{\omega}^{\mathrm{B}}_{\mathrm{B}/I}$ represents the angular velocity vector of the B-Frame with respect to the I-Frame, expressed in the B-Frame. The angular velocity propagation equation can be derived by differentiating the angular momentum equation, which relates torque to the rate of change of angular momentum. The resulting angular velocity propagation equation is represented as:

$$\dot{\boldsymbol{\omega}}^{\boldsymbol{B}}_{\boldsymbol{B/I}} = (J^B)^{-1}\left(\boldsymbol{\tau}^{\boldsymbol{B}}_{\boldsymbol{c}} - \boldsymbol{\omega}^{\boldsymbol{B}}_{\boldsymbol{B/I}} \times \mathbf{h}^{\mathbf{B}}\right), \tag{3}$$

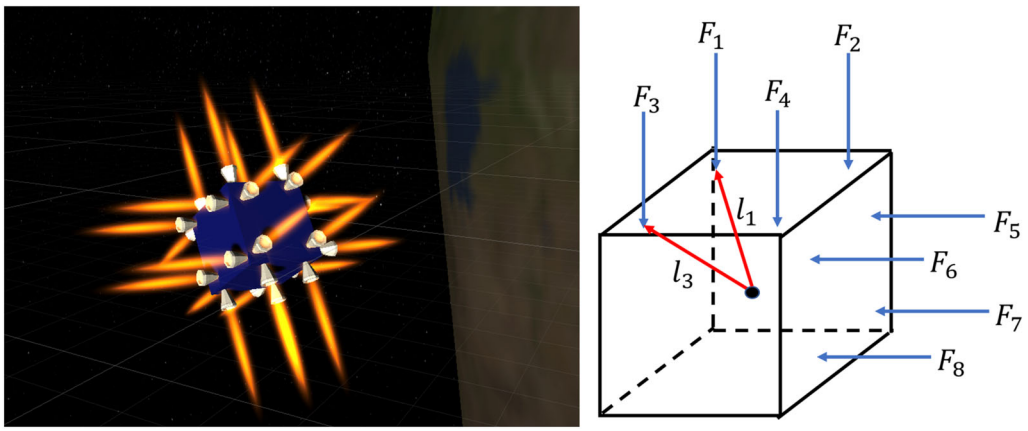

Fig. 2 Thrusters configuration: **a** Spacecraft with 24 thrusters displaying the positions and the directions of the thrusters. **b** Notations for positions and thrust vectors of thrusters

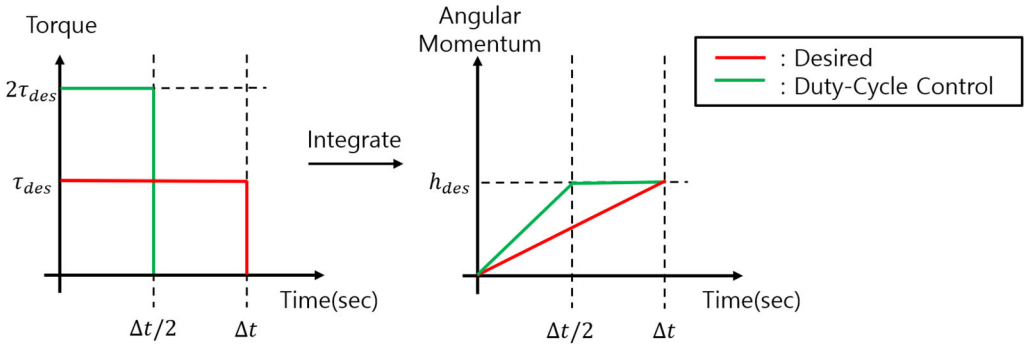

Fig. 3 Comparison of desired torque and angular momentum with duty-cycle control

Table 1 Reference frames

Name	Description	Definition
I-frame	Earth Centered Inertial Frame (ECI)	x: Direction to the vernal equinox
		y: $z \times x$
		z: Direction to the Earth's rotational axis
O-frame	Orbit Reference Frame (ORF)	x: $y \times z$
		y: Opposite to the orbital angular momentum
		z: Direction to the Earth's center
B-frame	Body Reference Frame (BRF)	Body-fixed to align with the O-frame
		in an Earth-pointing configuration

where J^B represents the moment of inertia (MOI) matrix expressed in the B-Frame, $\mathbf{h^B}$ denotes the angular momentum vector, and $\boldsymbol{\tau}_c^{\boldsymbol{B}}$ represents the torque due to the thrusters. It is assumed that the MOI matrix remains constant throughout the mission.

2.2.2 Orbital Dynamics

The translational motion describes the changes in the position and velocity of the spacecraft as it traverses its orbit. This study focuses solely on the thrust generated by the thrusters and the two-body dynamics between the Earth and the spacecraft, while other potential disturbances are neglected [16]. The equations of motion governing the position and velocity of the spacecraft can be expressed as:

$$\dot{\mathbf{x}} = \begin{bmatrix} \dot{\mathbf{r}} \\ \dot{\mathbf{v}} \end{bmatrix} = \begin{bmatrix} 0 & I \\ 0 & 0 \end{bmatrix} \begin{bmatrix} \mathbf{r} \\ \mathbf{v} \end{bmatrix} + \begin{bmatrix} 0 \\ I \end{bmatrix} \mathbf{a}, \tag{4}$$

$$\mathbf{a} = \frac{\mathbf{f}}{m} = \mathbf{a_{TB}} + \mathbf{a_{RCS}}, \tag{5}$$

$$\mathbf{a_{TB}} \approx -\mu_E \frac{\mathbf{r}}{\|r\|^3}. \tag{6}$$

In this formulation, $\mathbf{x}$ represents the state vector of the spacecraft, which comprises the position vector $\mathbf{r}$ and the velocity vector $\mathbf{v}$. The acceleration vector $\mathbf{a}$ is determined by the forces acting on the spacecraft, as described by Equation (5). Here, $\mathbf{f}$ denotes the total force acting on the spacecraft, and m is its mass. The term $\mathbf{a_{TB}}$ represents the acceleration due to the two-body gravitational force between the Earth and the spacecraft, which is approximated by Equation (6). Additionally, $\mathbf{a_{RCS}}$ denotes the acceleration due to the thrust produced by the reaction control system. The standard gravitational parameter for Earth is denoted by μ_E.

Understanding these variables and their interrelationships is crucial for accurately describing and predicting the spacecraft's motion and dynamics within its orbital environment. The equations of motion provide a comprehensive framework for analyzing the translational behavior of spacecraft under the combined influences of gravitational and thrust forces.

3 Controller Module

The Controller Module, a pivotal component in spacecraft attitude control systems, plays a critical role by determining the precise on-times of individual thrusters based on input parameters such as the desired attitude, current attitude, and current angular velocity. This module is composed of two integral components: the Attitude Controller and the Thruster Control Allocation algorithm.

The Attitude Controller utilizes a quaternion feedback regulator, a sophisticated tool that calculates the necessary torque to track the spacecraft's desired attitude. This choice of regulator is strategic, leveraging its robustness and computational efficiency in handling complex three-dimensional rotational dynamics. By effectively minimizing the discrepancy between the current and desired attitudes, the quaternion feedback regulator ensures precise and reliable attitude tracking, which is crucial for maintaining the spacecraft's trajectory and orientation within its operational environment.

The Thruster Control Allocation algorithm translates the calculated torque from the Attitude Controller into specific on-time commands for each thruster. This conversion is critical as it determines the precise duration each thruster must fire to achieve the required orientation adjustments. The algorithm employs a primal-dual interior point method, renowned for its effectiveness in solving medium-scale constrained optimization problems with high accuracy and computational efficiency. This optimization technique is particularly advantageous in the spacecraft context, where every second of thruster operation consumes valuable propellant and impacts the mission's overall efficiency and cost.

Furthermore, this method meticulously calculates the optimal thruster burn times needed to actualize the desired torque, thus ensuring optimal control allocation performance. The integration of the quaternion feedback regulator with the primal-dual interior point method forms a robust controller functionality that not only manages spacecraft attitude with high precision but also adapts dynamically to changing conditions in space. This dual-component approach ensures the spacecraft maintains its planned course and orientation, thereby enhancing mission reliability and success.

Through this sophisticated control architecture, the Controller Module effectively synchronizes the spacecraft's attitude control processes, facilitating smooth and efficient operation while navigating the challenging environment of space. By accurately tracking the desired attitude and generating the requisite torque through precisely calculated on-times for each thruster, the module underpins the overall control strategy essential for advanced space missions.

3.1 Attitude Controller

3.1.1 Quaternion Feedback Regulator

Quaternion feedback control is a well-established technique extensively utilized in spacecraft attitude control for its robustness and precision in managing rotational dynamics in three-dimensional space. In the realm of control allocation problems, where the accurate computation of torque commands is critical, quaternion feedback assumes a pivotal role. The specific formulation of quaternion feedback, as delineated in Eq. (7), provides a systematic approach to minimize attitude errors and ensure stable spacecraft orientation. This method effectively translates desired attitude commands into precise torque outputs, thus facilitating optimal performance of the thruster allocation. The technique and its applications in spacecraft control systems are further elaborated in [17], where the benefits and operational efficiency it brings to spacecraft dynamics are comprehensively discussed. The quaternion feedback control follows:

$$\boldsymbol{\tau}_{\text{cmd}}^{\boldsymbol{B}} = \left[\boldsymbol{\omega}_{\boldsymbol{B/I}}^{\boldsymbol{B}}\times\right] J^{B}\boldsymbol{\omega}_{\boldsymbol{B/I}}^{\boldsymbol{B}} - K_d\boldsymbol{\omega}_{\boldsymbol{B/I}}^{\boldsymbol{B}} - K_p\mathbf{q}_{\mathbf{I,e}}^{\mathbf{B}}, \tag{7}$$

with the control gain matrices given by:

$$K_d = k_d J^{B}, \quad K_p = k_p J^{B}. \quad k_p, k_d > 0. \tag{8}$$

In this equation, $\boldsymbol{\tau}_{\text{cmd}}^{\boldsymbol{B}}$ represents the torque command that needs to be achieved by the thrusters, and $\mathbf{q}_{\mathbf{I,e}}^{\mathbf{B}}$ denotes the attitude error expressed in quaternions. The attitude error can be expressed as,

$$\begin{bmatrix} q_{1e} \\ q_{2e} \\ q_{3e} \\ q_{4e} \end{bmatrix} = \begin{bmatrix} q_{4c} & q_{3c} & -q_{2c} & -q_{1c} \\ -q_{3c} & q_{4c} & q_{1c} & -q_{2c} \\ q_{2c} & -q_{1c} & q_{4c} & -q_{3c} \\ q_{1c} & q_{2c} & q_{3c} & q_{4c} \end{bmatrix} \begin{bmatrix} q_1 \\ q_2 \\ q_3 \\ q_4 \end{bmatrix}, \tag{9}$$

where the quaternion q_{ie}, q_{ic} and q_i represent the attitude error, the desired attitude, and the current attitude, respectively.

The quaternion feedback law presented in Equation (7) represents a form of a PD (Proportional-Derivative) controller, augmented with a nonlinear body-rate feedback term that cancels the gyroscopic coupling torque. This formulation incorporates feedback from both the quaternion error and angular velocity. The PD control gain parameters are denoted by k_p and k_d, which are critical for the proper tuning and performance of the control system, ensuring stability and responsiveness in the spacecraft's attitude control. It has been demonstrated that configuring the gain matrices as shown in (8) results in a stabilized attitude control system [17].

This configuration ensures that the control system can effectively manage the spacecraft's orientation, thereby enhancing its stability and robustness against external disturbances and internal uncertainties.

3.2 Thruster Control Allocation

3.2.1 Control Allocation Algorithm

The control allocation problem for the individual thrusters within the Reaction Control System (RCS) of a spacecraft is formulated as an optimization problem and addressed using convex optimization algorithms. This optimization task can be approached using two distinct methodologies: Linear Programming (LP) and Relaxed Quadratic Programming (QP). For effective resolution of this problem, the primal-dual interior point method is employed, noted for its efficiency and robustness in handling complex, medium-scale optimization tasks [13].

Rooted in the principles of convex optimization, this method offers substantial advantages, including guaranteed convergence to a global optimum. This is particularly crucial in ensuring that the control strategies devised are not only theoretically sound but also practically viable. Moreover, its capacity to manage multiple objectives simultaneously allows for a more nuanced and comprehensive approach to optimization. This capability is essential for maintaining the balance between competing demands, such as minimizing fuel consumption while maximizing maneuverability and stability of the spacecraft.

The use of convex optimization techniques ensures that the solutions derived are not only optimal but also computationally efficient. This efficiency is vital for real-time applications within spacecraft attitude control systems, where decisions must be made rapidly and reliably under varying and unpredictable conditions. The application of such sophisticated optimization frameworks significantly enhances the capability and reliability of spacecraft operations, ensuring optimal performance and responsiveness in critical situations.

3.2.2 Linear Programming

The control allocation problem can be formulated using linear programming. Linear programming is a potent mathematical technique designed to optimize a linear objective function, subject to a set of linear equality and inequality constraints. Within the context of the control allocation problem, LP offers a structured framework for determining the optimal thruster on-times that minimize fuel consumption while fulfilling the required control objectives. A key advantage of LP is its ability to guarantee a global optimum solution, a feature attributed to the convex nature of the problem.

Convex optimization techniques, such as the primal-dual interior point method utilized in this study, are especially adept at solving large-scale LP problems efficiently and reliably. These methods ensure that the solutions are not only optimal but also computationally efficient, making them ideal for real-time applications in spacecraft control systems. The primary objective of this optimization is to determine the optimal on-times for each thruster, thereby ensuring efficient fuel usage while achieving the desired control torques and forces. This problem can be mathematically expressed as,

$$\begin{aligned} &\text{minimize} && \mathbf{c}^T\mathbf{u} \\ &\text{subject to} && 0 \le \mathbf{u} \le \Delta t\mathbf{1}, \\ &&& A\mathbf{u} = \mathbf{d}_{\text{des}}, \end{aligned} \tag{10}$$

where

$$\mathbf{d}_{\text{des}} = \begin{bmatrix} \mathbf{F}_{\text{cmd}} \\ \boldsymbol{\tau}_{\text{cmd}} \end{bmatrix} \tag{11}$$

represents the vector of command signals passed from the attitude controller, and the one-vector $\mathbf{1}$ consists entirely of ones in each of its elements.

The objective function aims to minimize the total cost associated with the thruster burn times. In this formulation, $\mathbf{u}$ represents the vector of on-times for each individual thruster, and $\mathbf{c}$ is a vector of cost coefficients. The vector $\mathbf{c}$ represents the weighting parameters assigned to individual thrusters. By allocating higher weights to thrusters intended for infrequent use and lower weights to those permitted for more frequent operation, the utility frequency of each thruster can be systematically controlled. These coefficients typically correspond to factors such as fuel consumption, operational efficiency, or other mission-critical parameters. By minimizing this objective function, the optimization framework seeks to ensure the most efficient use of the limited fuel resources available on the spacecraft.

The constraints of the optimization problem are twofold. First, the inequality constraints ensure that the on-time for each thruster is non-negative and does not exceed the maximum allowable limit, such as the controller time step. These

constraints reflect the physical limitations of the thrusters. Second, the equality constraints guarantee that the combined effect of the thrusters' actions produces the required command, $\mathbf{F}_{\text{cmd}}$ and $\boldsymbol{\tau}_{\text{cmd}}$. The matrix A encapsulates the relationship between each thruster's action and the resulting forces and torques on the spacecraft, taking into account the configuration of the thrusters.

3.2.3 Relaxed Quadratic Programming

While the LP formulation efficiently identifies the optimal solution, it presents limitations. One significant drawback is that it fails to produce a feasible solution when the commanded signals exceed the maximum force and torque (or linear and angular momentum changes) that can be realistically achieved during the specified control step size, Δt. This limitation can pose challenges in scenarios where dynamic responses require higher output than the system's design capabilities, potentially impacting the effectiveness of the control strategy and the numerical stability of the allocation algorithm under extreme operational conditions.

To address this infeasibility issue, we reformulate the optimization problem using multi-objective quadratic programming as follows:

$$\begin{aligned} &\text{minimize} \quad \|W\,(A\mathbf{u}-\mathbf{d}_{\text{des}})\|_2^2+\|V\mathbf{u}\|_1 \\ &\text{subject to} \quad 0\le\mathbf{u}\le\Delta t\mathbf{1}. \end{aligned} \tag{12}$$

The objective function is designed to minimize the weighted sum of the squared errors and the ℓ_1-norm of the thruster on-time vector. Specifically, the first term of the objective function represents the weighted ℓ_2-norm of the error between the commanded and achieved forces/torques. The weighting matrix W enables control designers to prioritize specific axes (x, y, or z) for precise tracking of the commanded force/torque. The second term of the objective function introduces a regularization term to penalize large on-time solutions, thereby promoting sparsity and efficiency in the thruster actuations. The matrix V allows us to control the priority of each thruster's utilization and serves the similar role as the vector $\mathbf{c}$ in Equation (10). The constraints are the same as those used in the LP formulation, reflecting the physical limitations of the thrusters.

To enhance computational efficiency and reliability, we convert the optimization problem into a general quadratic form. The reformulated problem is specified as follows:

$$\begin{aligned} \text{minimize} \quad & \begin{bmatrix}\mathbf{u}\\ \mathbf{s}\end{bmatrix}^T \begin{bmatrix}A^TW^TWA & 0\\ 0 & 0\end{bmatrix}\begin{bmatrix}\mathbf{u}\\ \mathbf{s}\end{bmatrix} \\ & +\begin{bmatrix}-2A^TW^TWd_{\text{des}}\\ \mathbf{1}\end{bmatrix}^T\begin{bmatrix}\mathbf{u}\\ \mathbf{s}\end{bmatrix}. \end{aligned}$$

$$\text{subject to} \quad \begin{bmatrix}-I & 0\\ I & 0\\ -V & -I\\ V & -I\end{bmatrix}\begin{bmatrix}\mathbf{u}\\ \mathbf{s}\end{bmatrix}\le\begin{bmatrix}0\\ \Delta t\mathbf{1}\\ 0\\ 0\end{bmatrix}. \tag{13}$$

In this formulation, the variable vector is expanded to include both the original control inputs $\mathbf{u}$ and additional slack variables $\mathbf{s}$. The constraints are similarly extended to incorporate these slack variables, thus ensuring the feasibility and solvability of the problem within the specified physical limitations.

This reformulation leverages the strengths of quadratic programming to provide a more robust framework for optimizing thruster on-times under complex constraints. A significant advantage of this approach is its inherent feasibility; it replaces the hard constraint $A\mathbf{u}=\mathbf{d}_{\text{des}}$ with a soft constraint that is appended to the objective term, thereby enhancing the reliability of the spacecraft attitude control system. Furthermore, the inclusion of two weighting matrices, W and V, adds versatility to the problem formulation.

Additionally, this method benefits from the advanced solution techniques available for quadratic programming problems, ensuring computational efficiency and suitability for real-time applications in space operations.

3.2.4 Primal-Dual Interior Point Method

The aforementioned two forms of optimization problems can be solved using the primal-dual interior point method. This advanced optimization technique is particularly well-suited for handling medium-scale, constrained optimization problems, making it ideal for applications in spacecraft attitude control. See [13] for details on the solution methods.

The method is a sophisticated algorithm used for solving convex optimization problems, particularly those involving linear and quadratic programming. It operates by simultaneously considering the primal and dual residuals of the optimization problem, iteratively converging to the optimal solution. This method is highly efficient in dealing with medium-scale problems due to its polynomial-time complexity and robustness in navigating the feasible solution space. The algorithm starts with an initial feasible point within the interior of the feasible region and iteratively moves towards the optimal solution by following a path defined by the primal and dual search direction. By maintaining feasibility with respect to both the primal and dual problems, the method ensures convergence to a globally optimal solution. This is particularly advantageous in aerospace applications where precision and reliability are paramount.

In the context of the control allocation problem for spacecraft attitude control, this method offers several key benefits. It provides robustness by effectively managing complex constraints and consistently finding feasible solutions,

Fig. 4 Computation time for solving control allocation problems with varying numbers of thrusters

even under stringent operational conditions. Additionally, the method's polynomial-time complexity ensures that solutions are obtained swiftly, making it well-suited for real-time applications. Figure 4 illustrates the increase in computation time with increasing problem sizes when using the primal-dual interior point method. The results represent the average computation time for 100 executions of thrust allocation commands across cases involving 24, 36, 48, 60, 72, 84, and 90 thrusters. The growth in computation time is significantly slower than the $O(n^3)$ complexity typically associated with matrix inversion, highlighting the efficiency of the proposed method. Furthermore, the method is capable of efficiently addressing medium-scale optimization problems, which is crucial for systems that incorporate numerous control inputs and constraints, demonstrating significant scalability. By employing the primal-dual interior point method, we can ensure that the optimization problems for control allocation are solved accurately and efficiently, thereby enhancing the performance and reliability of the spacecraft attitude control system.

4 Numerical Experiments

We will conduct a series of numerical experiments to assess the effectiveness of the proposed attitude control and control allocation methods. These simulations will utilize both LP and the relaxed QP to approach the problem from different computational perspectives.

The simulation scenarios are organized into three distinct cases based on the angular maneuver scale: Case A, which involves a small angle maneuver, and Case B and C, which involve a large angle maneuver. The simulation parameters and initial conditions for each case are presented in Tables 2 and 3. The initial torque command is determined based on the initial conditions and the initial attitude command. Figure 5 illustrates the set of torque vectors achievable with the set of given thrusters, along with the initial torque command. The figure is rotated and displayed from different perspectives to provide a comprehensive view. From the results in Fig. 5, it is evident that the torque command is achievable only in Case A, while it is infeasible for Case B and Case C.

In Case A, the scenario entails a small angle maneuver where the commanded forces and torques remain within achievable limits throughout the entire maneuver mission. This ensures that the LP formulation remains feasible, allowing for smooth and effective control allocation throughout the maneuver. This case exemplifies situations where minimal adjustments are needed to align the satellite, making it ideal for assessing the efficiency and responsiveness of the control system under nominal conditions.

Conversely, Case B and C involve a large angle maneuver where the initially commanded forces and torques exceed the system's operational limits, rendering the LP formulation initially infeasible. This scenario presents significant challenges in accurately tracking the commanded forces and torques at the start of the maneuver. Case B and C are designed to test the system's ability to handle more extreme conditions, where substantial reorientation is required, and to evaluate the robustness and adaptability of the control allocation algorithms when dealing with significant deviations from the target states.

These simulations will be conducted under conditions simulating Earth-pointing maneuvers, a typical requirement for many satellite missions. This involves orienting the satellite's sensors and communication equipment towards Earth to maximize data acquisition quality and maintain robust communication links. The parameters and conditions assumed for this simulation study are designed to mimic realistic operational environments, providing a comprehensive evaluation of the control strategies under various operational stresses.

By simulating these contrasting scenarios, we aim to thoroughly assess the performance of the attitude control and control allocation methods across a spectrum of operational conditions, ranging from relatively favorable to significantly demanding. This comprehensive approach ensures that the control strategies are both theoretically sound and practically viable, capable of addressing a variety of real-world challenges.

4.1 Case A: Small Angle Maneuver

The simulation results for Case A using the LP formulation are illustrated in Fig. 6 through Fig. 9. Figure 6 displays the attitude and angular velocity of the satellite, where alignment of the O-Frame with the B-Frame indicates an Earth-pointing satellite as per the definitions of the coordinate systems. It

Table 2 Location and direction of thrust for each thruster

Thruster ID	Location of Thruster (x, y, z), in m	**Direction of Thrust** (x, y, z)
#1	0.5, 1, −0.7	0, -1, 0
#2	−0.9, 1, −0.8	0, -1, 0
#3	0.8, 1, 0.8	0, -1, 0
#4	−0.8, 1, 0.6	0, -1, 0
#5	0.6, -1, 0.9	0, 1, 0
#6	0.8, -1, 0.7	0, 1, 0
#7	−0.9, -1, −0.8	0, 1, 0
#8	−0.5, -1, 0.6	0, 1, 0
#9	1, 0.8, 0.8	-1, 0,0
#10	1, −0.6, −0.9	-1, 0, 0
#11	1, 0.4, −0.7	-1, 0, 0
#12	1, −0.7, 0.7	-1, 0, 0
#13	-1, 0.7, −0.6	1, 0, 0
#14	-1, −0.6, 0.8	1, 0, 0
#15	-1, 0.8, −0.7	1, 0, 0
#16	-1, −0.7, −0.7	1, 0, 0
#17	0.9, 0.6, 1	0, 0, -1
#18	−0.8, 0.7, 1	0, 0, -1
#19	0.7, −0.7, 1	0, 0, -1
#20	−0.8, −0.8, 1	0, 0, -1
#21	0.7, 0.8, -1	0, 0, 1
#22	−0.9, 0.6, -1	0, 0, 1
#23	−0.7, −0.7, -1	0, 0, 1
#24	0.8, −0.7, -1	0, 0, 1

Table 3 Parameters and initial conditions for simulations

Item	Value	Unit
Thruster force	10	N
Thruster position	See Table 2	–
Thrust direction	See Table 2	–
Mass (m)	2500	kg
Moment of inertia (J^B)	$\begin{bmatrix} 1200 & 100 & -200 \\ 100 & 2200 & 300 \\ -200 & 300 & 3100 \end{bmatrix}$	$\mathrm{kg\,m^2}$
Control gain parameters	$k_d = 0.2, k_p = 0.05$	–
Weighting matrices	$W = I, V = I, \mathbf{c} = \mathbf{1}$	–
Initial attitude ($\mathbf{q}_\mathbf{I}^\mathbf{B}$, Case A)	(0.404, −0.493, 0.204, 0.743)	–
Initial attitude ($\mathbf{q}_\mathbf{I}^\mathbf{B}$, Case B)	(0.57,0.57,0.57,0.159)	–
Initial attitude ($\mathbf{q}_\mathbf{I}^\mathbf{B}$, Case C)	(0.156,−0.598,0.689,0.377)	–
Initial angular velocity ($\boldsymbol{\omega}_{\boldsymbol{B/I}}^{\boldsymbol{B}}$)	(0.01,0.01,0.01)	rad/s
Control time interval (Δt)	1	sec

is observed that the satellite's attitude stabilizes with Earth alignment at approximately 40 s, and angular velocity convergence follows at about 50 s.

Figure 7 compares the commanded torque with the actual torque. The graphs for the x, y, and z axes are displayed from left to right. It is challenging to determine the accuracy of control allocation solely from Fig. 7.

Figure 8 compares the product of the torque command and the control time interval with the product of the actual torque and the duration of burn. Since the duty-cycle control is used in this study, it is essential to verify whether the desired angu-

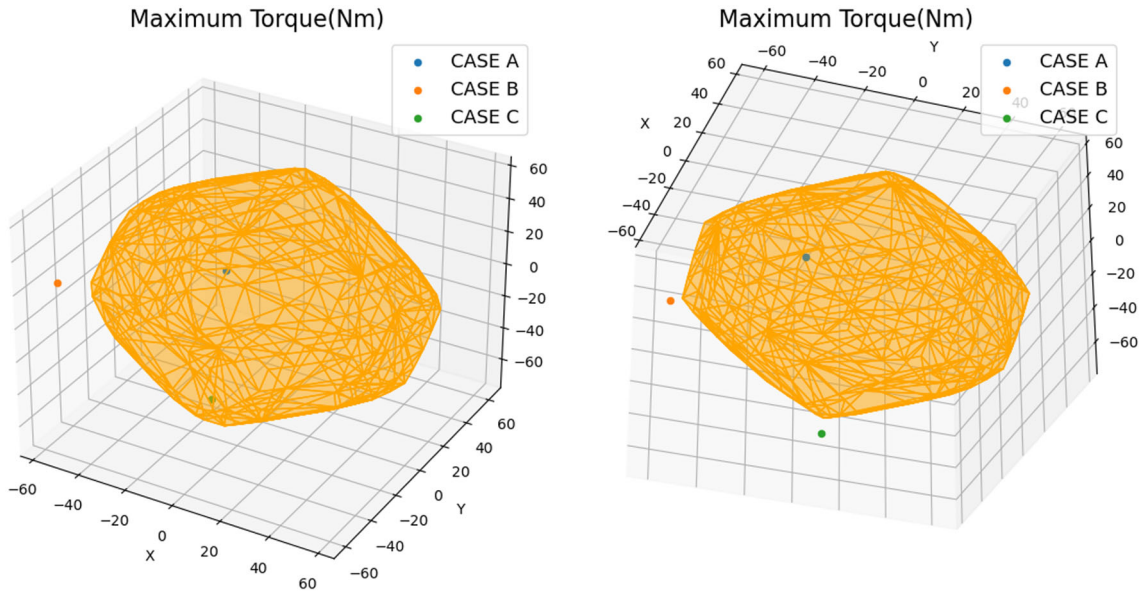

Fig. 5 Set of achievable torque vectors and initial torque commands. Note that the initial torque command lies within the feasible set only in Case A

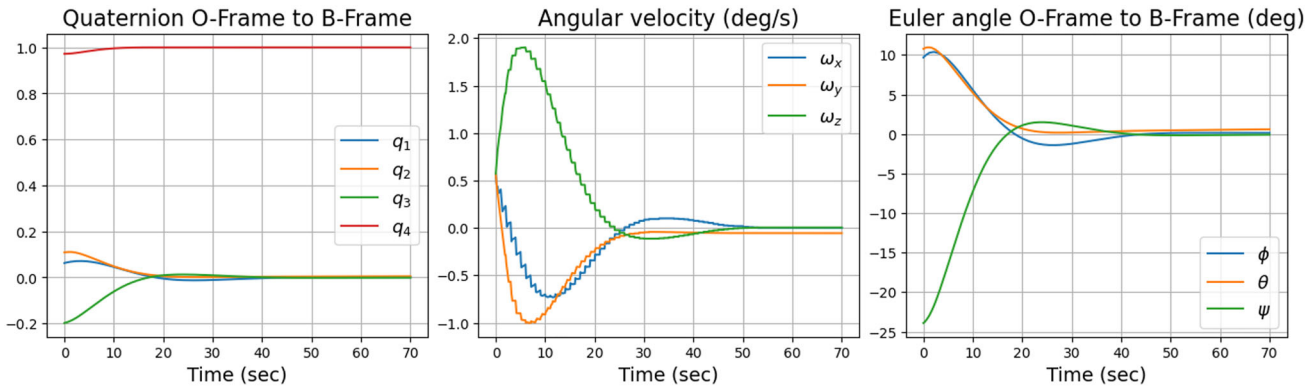

Fig. 6 Attitude and angular velocity for Case A from LP formulation: quaternion, angular velocity, and Euler angles

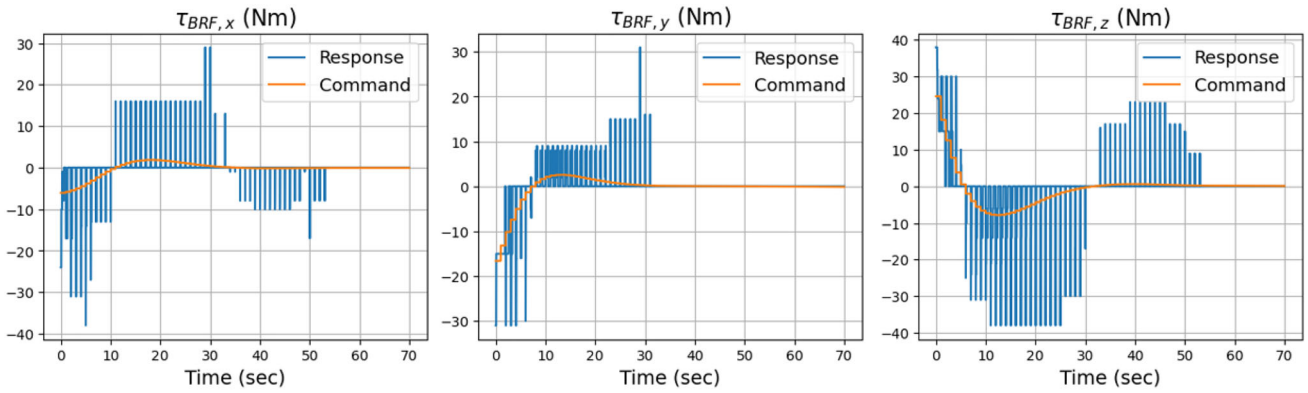

Fig. 7 Comparison of commanded versus achieved torque for Case A from LP formulation

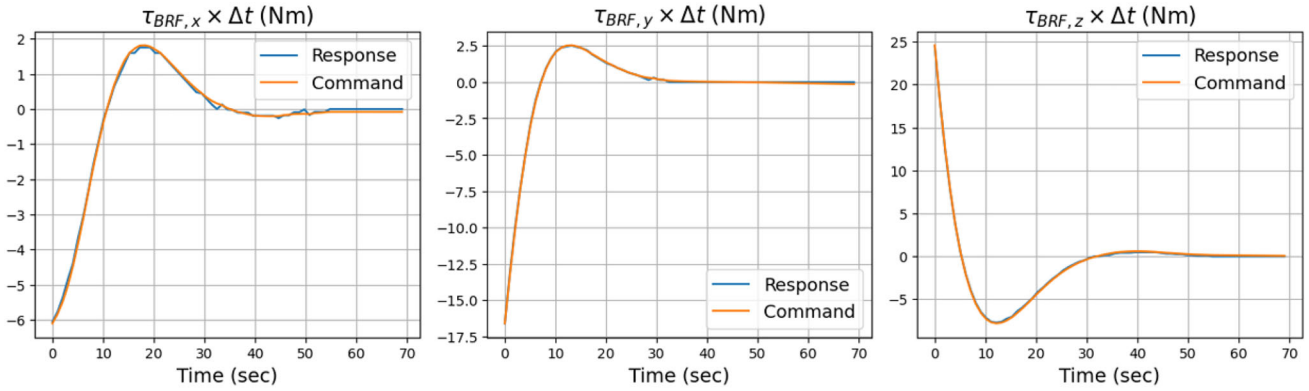

Fig. 8 Comparison of commanded versus achieved angular momentum changes for Case A using LP formulation

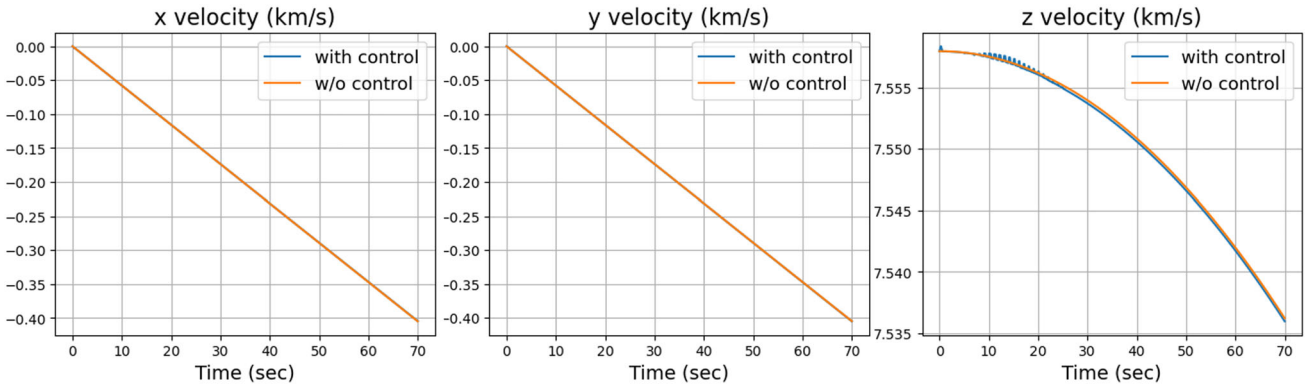

Fig. 9 Orbital velocity for Case A using LP formulation

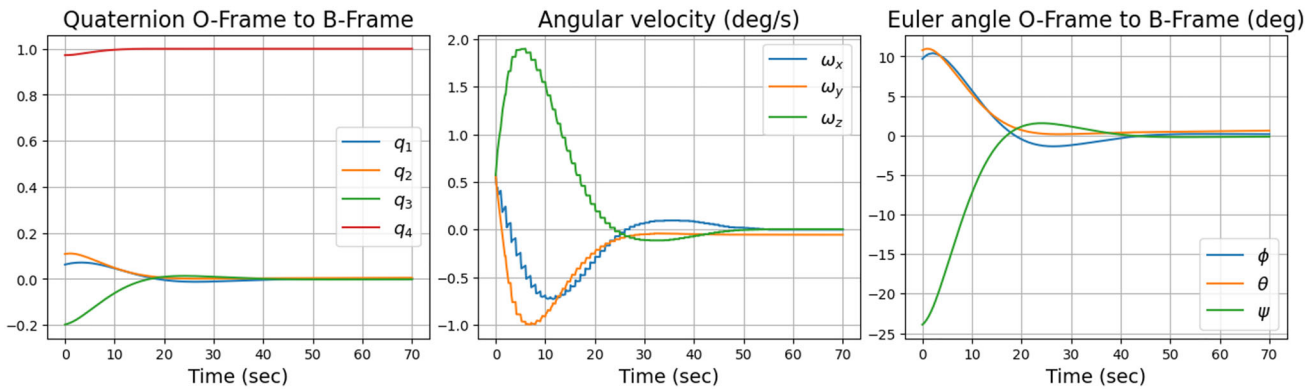

Fig. 10 Attitude and angular velocity for Case A from relaxed QP formulation: quaternion, angular velocity, and Euler angles

lar momentum is achieved. Torque represents the change in angular momentum, so the area under the torque graph represents the angular momentum. Figure 8 shows a comparison of these areas for each time step, indicating that the actual and desired areas match closely, confirming proper control allocation.

Figure 9 displays the velocity of the satellite. When using the RCS for attitude control, asymmetric thruster activation due to the duty-cycle implementation and the granularity of control due to the minimum on-time unit can result in a net thrust that is not zero, despite a zero desired net force. If this net thrust is too large, it can alter the satellite's orbit. Figure 9 confirms that the orbit remains largely unchanged, indicating effective control.

The simulation results for Case A using the relaxed QP approach are depicted in Figs. 10 11, 12 and 13. Overall, the results are very similar to those obtained using the LP approach, with only minor discrepancies noted in the torque values.

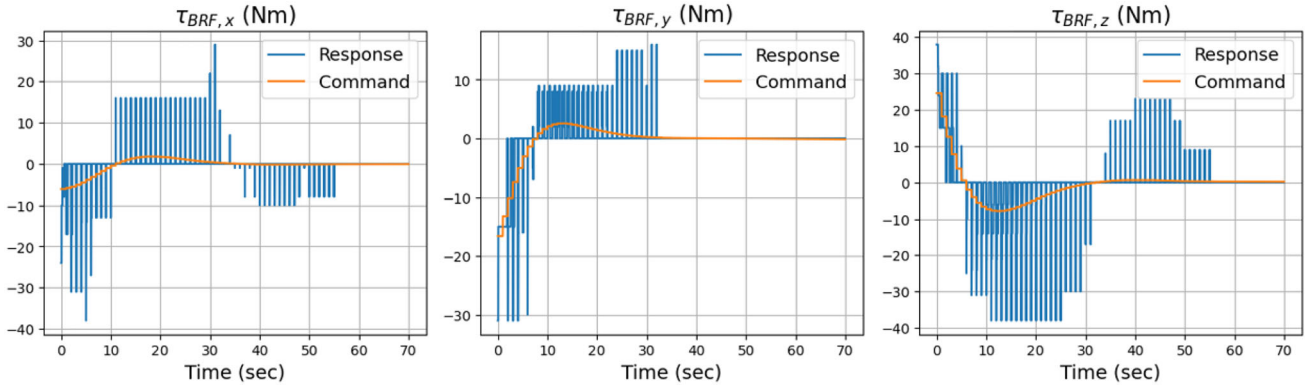

Fig. 11 Comparison of commanded versus achieved torque for Case A from relaxed QP formulation

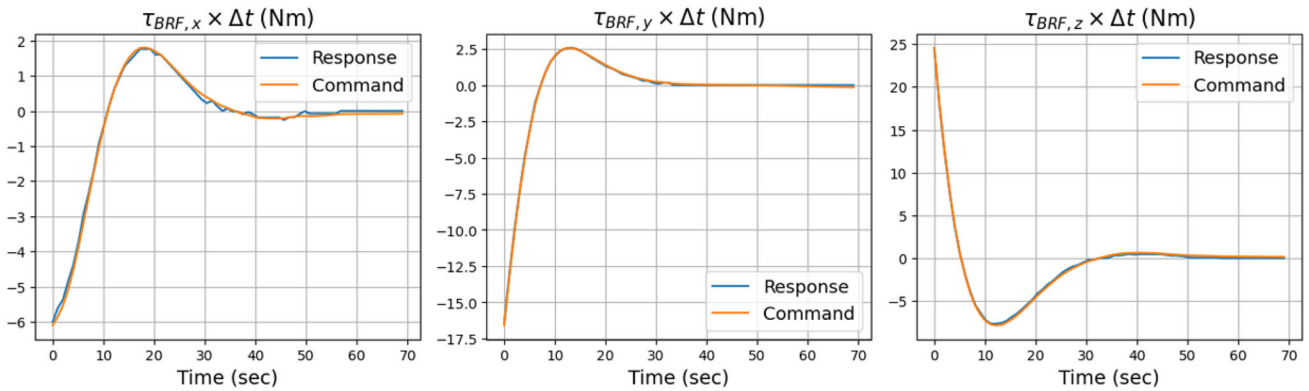

Fig. 12 Comparison of commanded versus achieved angular momentum changes for Case A using relaxed QP formulation

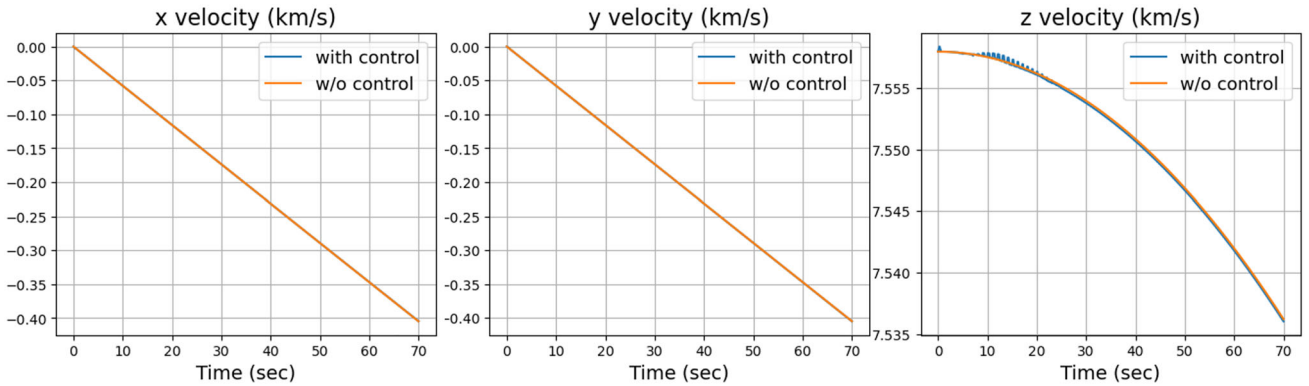

Fig. 13 Orbital velocity for Case A using relaxed QP formulation

4.2 Case B and C: Large Angle Maneuver

Since Case B involves a large angle maneuver that demands an excessive initial torque beyond the capacity of the thruster setup, the LP formulation becomes infeasible. The simulation results for Case B, employing a relaxed QP approach, are presented in Fig. 14, 15, 16 and 17.

Figure 14 illustrates the attitude and angular velocity of the satellite. Notably, by around 50 s, the satellite successfully achieves both angular velocity damping and Earth-pointing. This result verifies the effectiveness of the control strategy, demonstrating its capability to correct the satellite's attitude from initially infeasible conditions to the desired orientation.

Figure 15 compares the commanded and actual torques. Initially, the actual torque does not meet the commanded levels due to the infeasible starting conditions, underscoring the system's limitations in high-demand scenarios. However, as the simulation progresses, the actual torque increasingly aligns with the commanded torque, suggesting that the algorithm adeptly adjusts to initially challenging conditions.

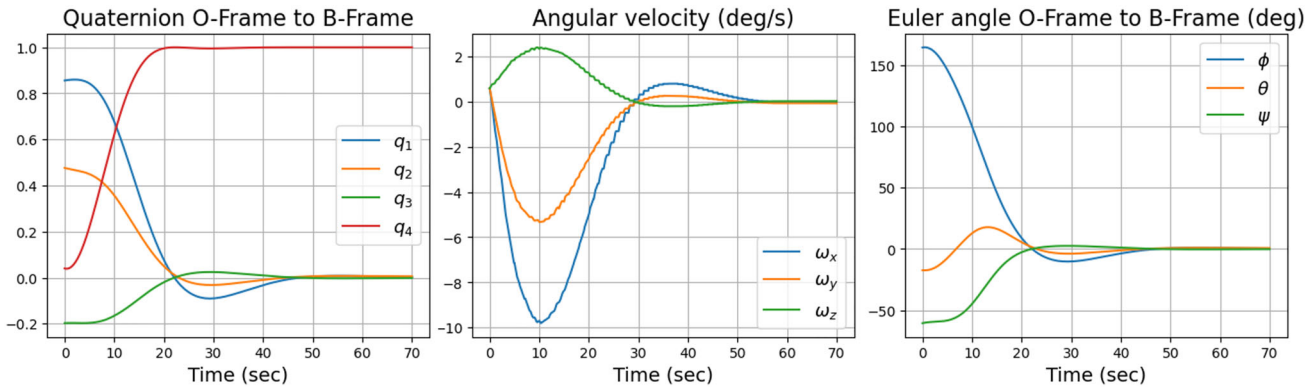

Fig. 14 Attitude and angular velocity for Case B from relaxed QP formulation: quaternion, angular velocity, and Euler angles

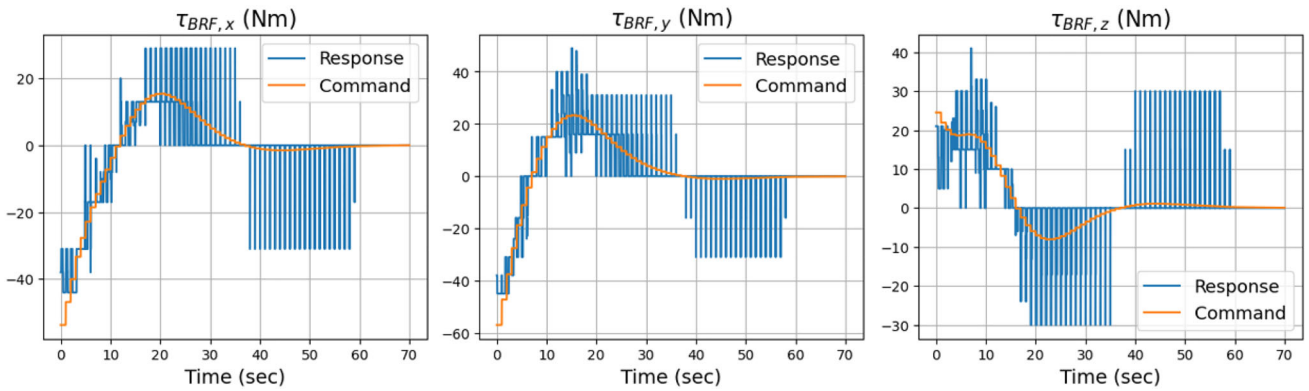

Fig. 15 Comparison of commanded versus achieved torque for Case B from relaxed QP formulation

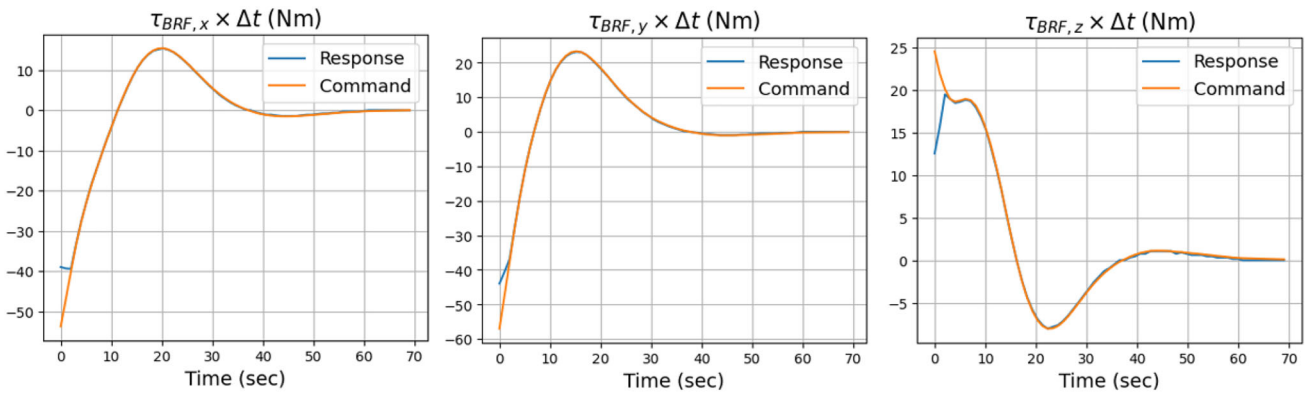

Fig. 16 Comparison of commanded versus achieved angular momentum changes for Case B using relaxed QP formulation

Figure 16 provides a deeper examination of this mechanism by comparing the product of the torque command and the control time interval with the product of the actual torque and the duration of its application. This comparison effectively measures the required versus achieved changes in angular momentum for this application, offering a clear visualization of how closely the system meets the performance criteria under varying conditions. Early in the simulation, the commanded torque levels are unattainable, but as the satellite's attitude is corrected, the system begins to accurately track the commanded torque. The convergence of the areas under the torque curves over time signals successful control allocation and effective momentum management.

Figure 17 shows the satellite's velocity, revealing a slight but not substantial deviation compared to Case A. This minor difference suggests that while asymmetric thruster forces slightly impact the satellite's orbit, these effects are not significant enough to notably alter its trajectory. Moreover, should substantial orbital deviations occur, adjustments to the force commands within the objective function are expected

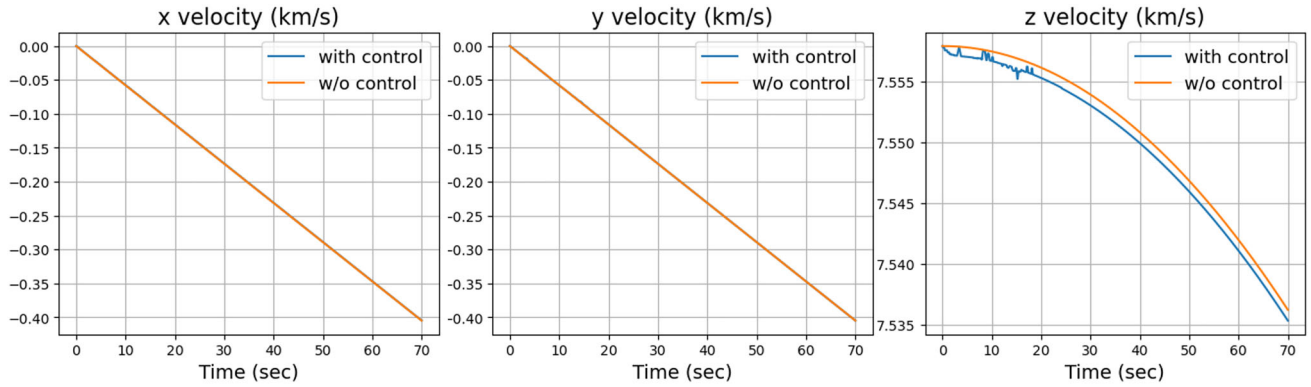

Fig. 17 Orbital velocity for Case B using relaxed QP formulation

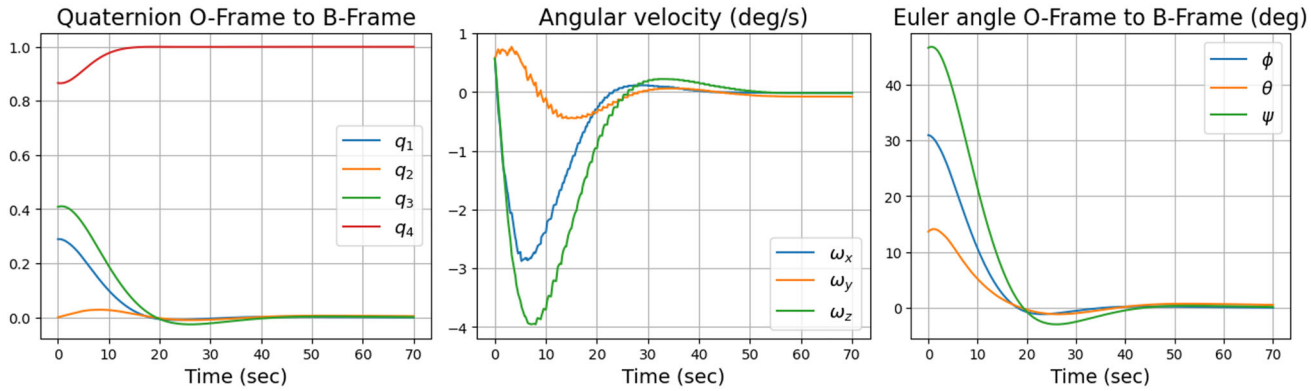

Fig. 18 Attitude and angular velocity for Case C from relaxed QP formulation: quaternion, angular velocity, and Euler angles

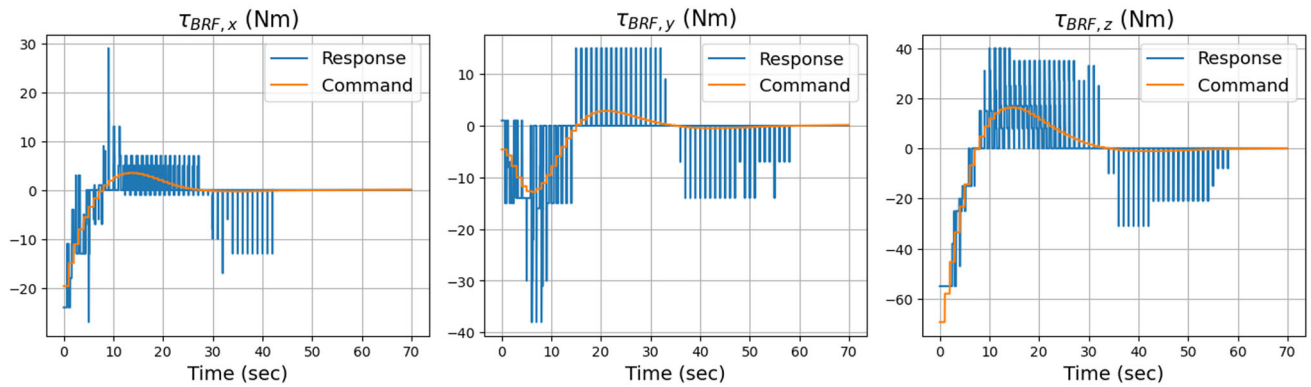

Fig. 19 Comparison of commanded versus achieved torque for Case C from relaxed QP formulation

to effectively correct the trajectory, further demonstrating the robustness of the control allocation algorithm in managing even challenging maneuver conditions.

Similarly, Case C involves a large-angle maneuver, with the results presented in Figs. 18, 19, 20, and 21. Since the scenario in Case C cannot be resolved using LP, only the Relaxed QP method was employed. Consistent with the observations in Case B, the attitude command successfully converged, and the torque command was accurately tracked. These results confirm that the Relaxed QP approach effectively handles control force allocation even in complex scenarios.

Figure 22 illustrates the number of thrusters utilized when the ℓ_2-norm and ℓ_1-norm regularizers are applied to the second term of the cost function in the Relaxed QP for Case B. Plot (a) shows the number of thrusters used over time, while plot (b) presents the usage per thruster across the entire simulation. The results indicate that the solution obtained with the ℓ_1 regularizer requires fewer thrusters, demonstrating

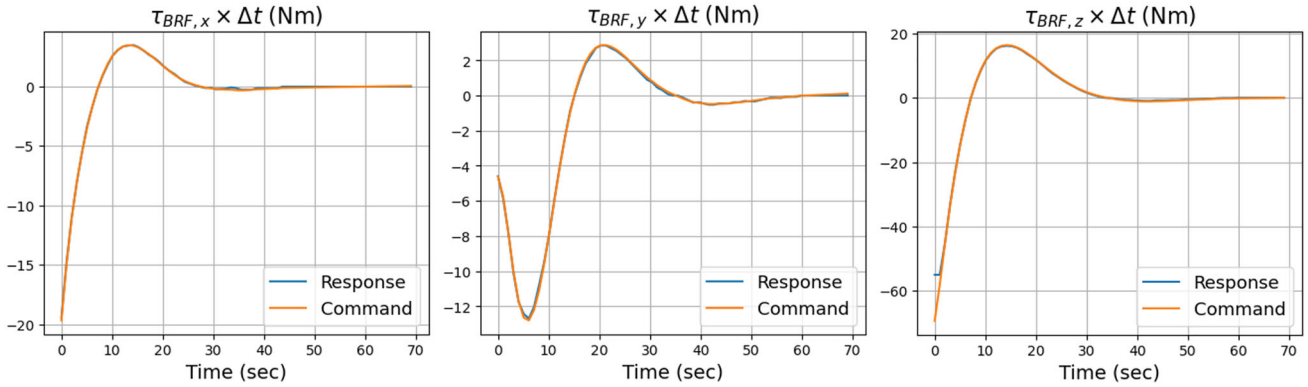

Fig. 20 Comparison of commanded versus achieved angular momentum changes for Case C using relaxed QP formulation

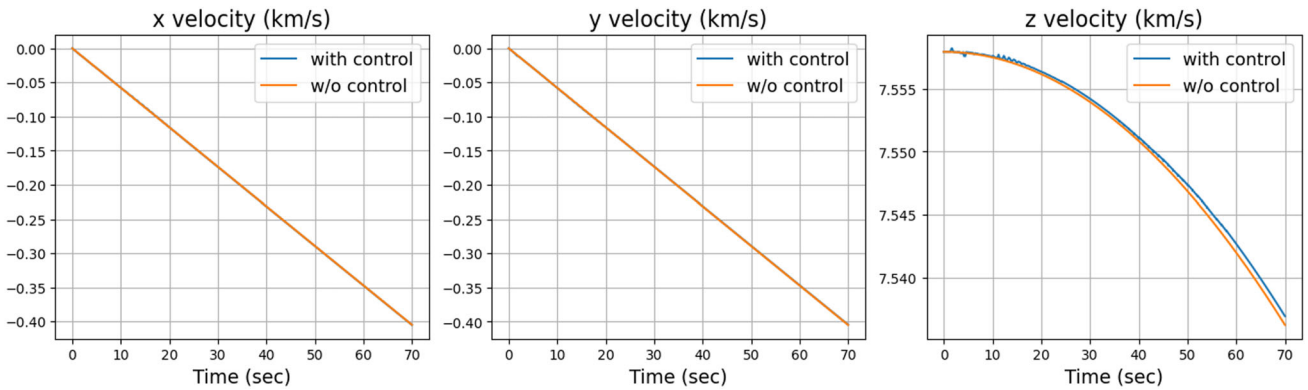

Fig. 21 Orbital velocity for Case C using relaxed QP formulation

improved operational efficiency with the Relaxed QP when using the ℓ_1 regularizer.

The simulation results for Case A, B and C provide valuable insights into the performance of the control allocation algorithm under different initial conditions. For Case A, both the LP approach and the relaxed QP approach demonstrated effective attitude control, with minor differences observed in the torque values. The satellite achieved Earth-pointing and angular velocity damping within the expected time frame. In contrast, Case B and C presented an infeasible scenario where the LP approach could not provide a solution. However, the relaxed QP approach successfully managed the initial infeasibility, gradually correcting the attitude and achieving the desired control. Despite initial discrepancies in the torque commands, the system adjusted over time, minimizing the impact on the satellite's orbit. These results underscore the relaxed QP algorithm's capability to handle both feasible and infeasible conditions, maintaining stability and effectiveness even under challenging scenarios. The findings suggest that with appropriate adjustments to the force commands in the objective function, the algorithm can correct significant orbital deviations, ensuring optimal performance and mission success.

5 Concluding Remarks

This study embarked on a rigorous evaluation of a newly proposed control allocation algorithm for spacecraft attitude control, employing linear programming (LP) and the relaxed quadratic programming (QP) across a series of detailed numerical experiments. These simulations were designed to probe the algorithm's performance under two distinct maneuver scenarios: Case A, involving small angle maneuvers, and Case B, involving large angle maneuvers.

In Case A, the control challenges were minimal, with the commanded forces and torques well within the operational capabilities of the spacecraft's Reaction Control System (RCS). The results demonstrated that both LP and the relaxed QP effectively maintained control, with the spacecraft's attitude and angular velocity stabilizing to desired parameters efficiently. The similarity in outcomes between LP and the relaxed QP, despite minor discrepancies in torque values, affirmed the robustness of the proposed methods under nominal conditions.

Conversely, Case B presented a more daunting challenge with initial conditions that far exceeded the thrusters' capacity, rendering the LP approach infeasible. However, the relaxed QP method excelled even under these stringent

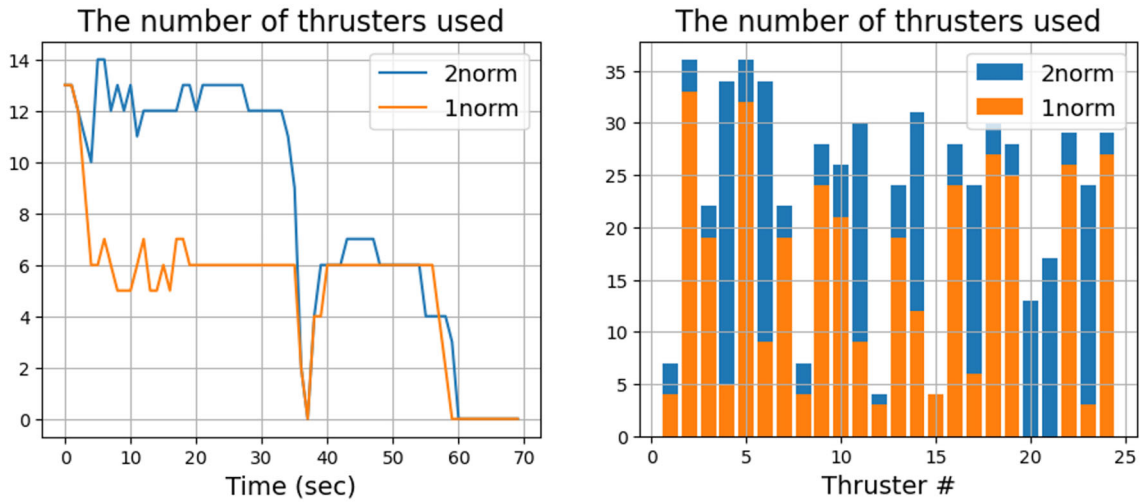

Fig. 22 Number of thrusters utilized: **a** Thruster count over time. **b** Usage per thruster

conditions, gradually aligning the spacecraft's attitude to achieve the required orientation and control. The progression of the actual torque to meet the commanded levels over time highlighted the adaptive capability of the control strategy to overcome initial infeasibilities. Furthermore, the detailed analysis of torque and angular momentum in Case B showcased the precision of the relaxed QP method in achieving and maintaining the desired control objectives. Despite initial discrepancies, the system effectively managed to align the actual torque with the commanded values as adjustments were made, illustrating the dynamic efficacy of the control algorithm.

Overall, the simulations confirmed the effectiveness of the proposed control allocation algorithm across a spectrum of operational scenarios, from relatively straightforward to highly demanding. The algorithm not only proved to be theoretically sound but also practically viable, ensuring stable spacecraft attitude control and minimal impact on orbital trajectories under varied and challenging conditions. These findings underscore the potential of the proposed methods to enhance the operational reliability and efficiency of spacecraft missions. Future research will aim to expand on these foundations, exploring additional optimization techniques and real-time control strategies to further refine and optimize spacecraft attitude control systems.

Funding This work was in part supported by KRIT grant funded by the Korea government (DAPA) (No. KRIT-CT-22-030, Reusable Unmanned Space Vehicle Research Center, 2024), and in part by the National Research Foundation of Korea funded by the Ministry of Science and ICT under Grant NRF-2022M1A3C2076483 (Space HR&D Center).

Data availability The datasets generated and/or analyzed during the current study are available from the corresponding author on reasonable request.

Declarations

Conflict of interest On behalf of all authors, the corresponding author states that there is no Conflict of interest.

References

1. Show L-L, Juang J-C, Jan Y-W (2003) An lmi-based nonlinear attitude control approach. IEEE Trans Control Syst Technol 11(1):73–83
2. Wei W, Wang J, Zuo M, Liu Z, Du J (2014) Chaotic satellite attitude control by adaptive approach. Int J Control 87(6):1196–1207
3. Barman S, Sinha M (2023) Satellite attitude control using double-gimbal variable-speed control moment gyroscope: single-loop control formulation. J Guid Control Dyn 46(7):1314–1330
4. Doman DB, Gamble BJ, Ngo AD (2009) Quantized control allocation of reaction control jets and aerodynamic control surfaces. J Guid Control Dyn 32(1):13–24
5. Song J, Cai G, Chen X (2018) Control allocation-based command tracking-control system for hypersonic re-entry vehicle driven by hybrid effecters. J Aerosp Eng 31(4):04018031
6. Servidia PA, Pena RS (2005) Spacecraft thruster control allocation problems. IEEE Trans Autom Control 50(2):245–249
7. Kishore WA, Dasgupta S, Ray G, Sen S (2013) Control allocation for an over-actuated satellite launch vehicle. Aerosp Sci Technol 28(1):56–71

8. Jin J, Park B, Park Y, Tahk M-J (2006) Attitude control of a satellite with redundant thrusters. Aerosp Sci Technol 10(7):644–651
9. Oppenheimer MW, Doman DB, Bolender MA (2006) Control allocation for over-actuated systems. In: 2006 14th mediterranean conference on control and automation. IEEE, pp 1–6
10. Lang X, Ruiter A (2021) Distributed optimal control allocation for 6-dof spacecraft with redundant thrusters. Aerosp Sci Technol 118:106971
11. Johansen TA, Fossen TI (2013) Control allocation—a survey. Automatica 49(5):1087–1103
12. Bodson M (2002) Evaluation of optimization methods for control allocation. J Guid Control Dyn 25(4):703–711
13. Boyd SP, Vandenberghe L (2004) Convex optimization. Cambridge University Press, Cambridge
14. Xie Y, Chen C, Liu T, Wang M (2021) Guidance, navigation, and control for spacecraft rendezvous and docking: theory and methods. Springer, New York
15. Markley FL, Crassidis JL (2014) Fundamentals of spacecraft attitude determination and control. Springer, New York
16. Vallado DA (2001) Fundamentals of astrodynamics and applications, vol 12. Springer, New York
17. Wie B, Weiss H, Arapostathis A (1989) Quarternion feedback regulator for spacecraft eigenaxis rotations. J Guid Control Dyn 12(3):375–380